



Contents lists available at ScienceDirect

Advanced Powder Technology

journal homepage: www.elsevier.com/locate/apt

Original Research Paper

Segregation pattern of binary-size mixtures in a double-walled rotating drum

S.H. Chou, L.T. Sheng, W.J. Huang, S.S. Hsiau *

Department of Mechanical Engineering, National Central University, Jhongli 32001, Taiwan, ROC

ARTICLE INFO

Article history:

Received 17 July 2019

Received in revised form 27 September 2019

Accepted 3 October 2019

Available online xxxxx

Keywords:

Rotating drum

Rotation speed

Segregation pattern

Granular temperature

ABSTRACT

Size-induced granular segregation was performed systematically and experimentally in an almost fully filled double-walled rotating drum at 10 different rotation speeds and two different side wall types. The motion of the granular materials was recorded using a high-speed camera for image analysis of particle segregation development in the drum. With continual tracking of the particle movements, the velocity, fluctuations, and granular temperatures were measured. The experimental results indicate that both rotation speeds and friction coefficient of side walls significantly affect segregation phenomena in binary-size mixture granular flows. The results demonstrate similar situations to the Brazil-nut effect and its reverse in the radial direction at either high or a low rotational speed (where the Froude number (Fr) is far from 1). At these instances, the maximum granular temperature occurs near the side walls. Specifically, a double segregation effect (DSE) is found at Froude number (Fr) close to 1. These results can be used in many industrial processes, for example, size grading of materials, screening of impurities, and different structures of functionally graded materials. Moreover, the maximum granular temperature occurs in the middle of the ring space. It causes small particles to move toward both side walls as it pushes bigger particles to accumulate in the middle of the ring space of rotating drum.

© 2019 The Society of Powder Technology Japan. Published by Elsevier B.V. and The Society of Powder Technology Japan. All rights reserved.

1. Introduction

Powder mixing is an essential industrial and household process that involves the realization of a proper mixture of different granular raw materials to ensure high quality of a product or semi-product. This process is very crucial in many industries such as pharmaceuticals, foodstuffs, ceramics, chemicals, and plastics. Regardless of the particle size, when more than one kind of particles co-exist in a system, segregation occurs between the particles as they move; for example, in the pharmaceutical industry where concoction and segregation of drugs and medicinal ingredients need to be executed precisely. Thus, industrial engineers and academic researchers have been investigating the fundamental mechanisms of mixing/segregation in powder or granular materials [1–3].

Segregation of granular mixtures can be achieved by mechanical excitation, gas-flow agitation, gravity-driven free falling, and many other different complex methods [4] due to differences in size, density, or shape. In the past few years, rotating drums have been widely used for the investigation of the mechanics of granular

flow and mixing/segregation, partly because the flow field in such drums is relatively simple [5–7]. In particular, two important flow regions exist in the granular material of a rotating drum: (i) a bulk solid-body region where the granular material undergoes slow plastic deformation, and (ii) a thin flowing layer that occurs when the rotating drum is less than half-filled with particles. Physical processes occur mainly in the flowing layer. In the rotating drum, the granular flow behavior can be separated into several flow regimes based on the particle motion. Moreover, the particle flow behavior and mixing/segregation mechanisms may be different in each flow regime. Thus, six identifiable flow regimes are used to describe particle motion in a rotating drum under different operational conditions of rotational speed, wall friction coefficient, filling degree, and so on such as slipping, slumping, rolling, cascading, cataracting, and centrifuging [8,9].

In a rotating drum with a binary granular mixture of particles with different sizes, segregation occurs as smaller particles fall between the voids among the particles, thus forming a core area in the drum center. This mechanism is known as percolation effect [10–12]. Moreover, segregation occurs in a binary mixture system with different densities due to buoyancy effect, where denser particles tend to sink to a lower level in the flowing layer to form a core at the drum center [13–15]. Thomas [16] studied the size

* Corresponding author.

E-mail address: sshsiau@cc.ncu.edu.tw (S.S. Hsiau).

segregation effect and found that, for smaller size ratios, segregation of large beads occurs at the surface of the flowing phase, whereas for higher size ratios, they are segregated into the core position. Arntz [17] used a discrete element method (DEM) to analyze the radial segregation phenomena in a rotating drum due to size effect. The results showed a strong correlation between the flow regime and the segregation pattern as the filling degree and the rotation speed were changed. In the past few years, our team has also carried out a series of studies on this topic [18–20].

When the rotating drum is approximately half-filled, granular segregation may change from the core segregation pattern to a streak segregation pattern [21,22]. Khakhar et al. [14] investigated different-sized particles and observed that streak formation usually occurs at low rotation speeds. Additionally, they indicated that radially segregated profiles for mixtures of different-sized particles reveal double segregation and complex dependence on the size ratio. Pereira et al. [23] also applied DEM to investigate radial streak patterns in a slowly rotating drum and discovered the necessity of the temporal fluctuations of the granular bed in the formation of streaks. Moreover, Liao et al. [24] discovered that dimensionless differences in the dynamic repose angle and density ratio strongly affect streak segregation patterns caused by density. They provided a phase diagram to identify the three pattern regimes of core segregation, streak segregation, and mixing.

Subsequently, when the rotating drum is more than half-filled, an unmixed region known as creeping region appears and rotates ideally along with the drum. In this phenomenon, the core has a faster rotation speed than that of the drum while its radius decreases with time [25–27], thereby the unmixed region causing longer time to achieve well mixing or segregation. In the case of the drum that is almost full, Turner and Nakagawa [28] found that the insufficient space restricts the movement and migration of different-sized particles. Meanwhile, Huang et al. [29] employed 3D DEM to investigate the segregation of a binary mixture in a fully filled rotating drum. They discovered that differences between the particle size and density ratios allow the segregation state to be quantified and illustrated on a phase diagram. Therefore, some researchers have proposed a double-walled rotating drum to effectively prevent the occurrence of bad segregation intensities and rates. Huang et al. [30] conducted a DEM simulation of a binary mixture in a double-walled rotating drum and reported that different self-gravity and centrifugal force predominantly determined the segregation behavior.

From the above discussion, although mixing or segregation based on size effect of particles has received considerable attention in the past few decades, several physical mechanisms are still unknown or poorly understood. Moreover, the double-walled rotating drum is a special system that was rarely discussed in the past. Therefore, this study consists of experiments to investigate the revolution and behavior of size-induced particle segregation in a quasi-two-dimensional double-walled rotating drum of different rotation speeds and side wall conditions.

2. Experimental procedure

Fig. 1 shows a schematic of the quasi-2D double-walled rotating drum whose axial length (δ) as well as outside and inside wall diameters are 15, 300, and 180 mm, respectively. Two different side wall conditions (acrylic and sandpaper) were used in this study. The rear surface of the drum was an aluminum plate that reduces electrostatic effects. It was adhered with a black paper to minimize optical noise effect in the digital images. A clear acrylic front plate was placed for flow visualization. Owing to the wall friction effect, the concentration profiles near the walls may differ from those in the bulk material. Thus, the front and rear walls of

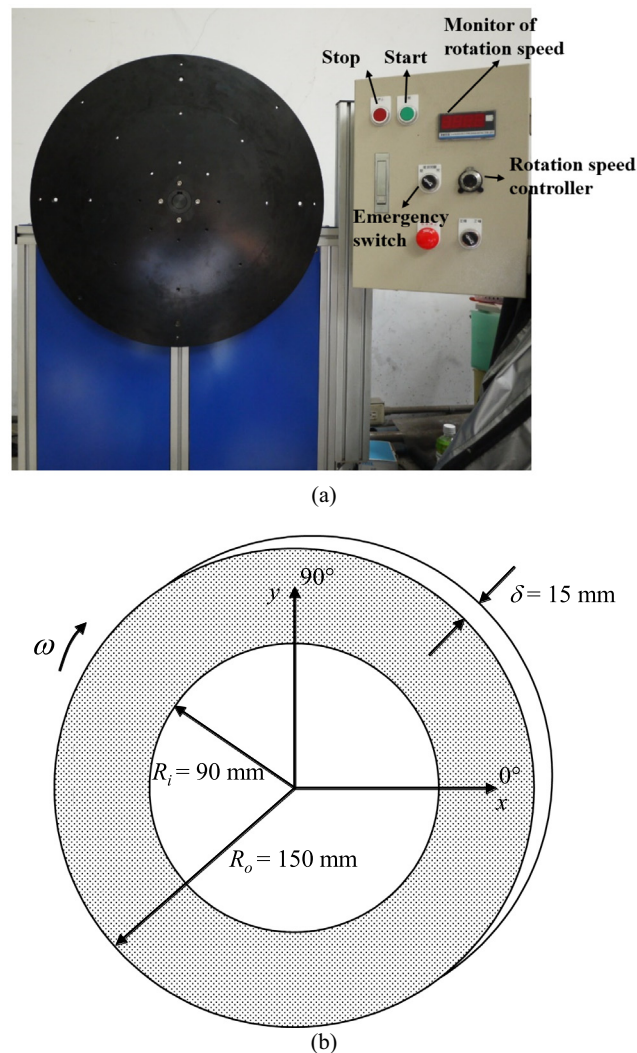


Fig. 1. Schematic diagram of (a) double-walled rotating drum, and (b) tank.

the drum were cleaned prior to each test to ensure that they were smooth and to reduce wall friction effect between the wall and the granular flows.

A stepper motor and micro series driver combination were used to rotate the drum at 7.326–8.687 rad/s, corresponding to the Froude number ($Fr = R\omega^2/g$) of 0.82–1.15, where ω is the drum angular velocity ($2\pi/T$, where T is the rotation period), R is the drum radius, and g is the acceleration due to gravity. The Froude number (Fr) is a dimensionless number defined as the ratio of the flow inertia to the external field. In this study, the Froude number was used to indicate the ratio of the centrifugal force to the gravitational force. The dimensionless axial thickness of the drum, defined as the ratio of the drum axial length to the big particle diameter, was set to 3.75. Two spherical glass beads with diameters 4 mm (black) and 2 mm (white) with a particle size ratio (d^*) of 2 were used for all the experiments. The standard deviation of the bead diameter was 0.09 mm while the bead density was 2.476 g/cm³. In all the experiments, the filling degree (f) of the granular materials was 0.94, and the volume ratio of the bigger and smaller glass beads was 50–50%. The details of the experimental conditions are provided in Table 1.

A Sony HDR-XR550 camera with a speed of 30 frames per second (fps) and a spatial resolution of 1280 × 1024 pixels was used to record flow images during the segregation process. Moreover,

Table 1

Experimental parameters. Particles are glass beads ($\rho_p = 2476 \text{ kg/m}^3$) with nominal diameters of 4 mm (large) and 2 mm (small).

Case	ω (rad/s)	Fr	Side wall type
1	7.326	0.82	acrylic
2	7.641	0.89	acrylic
3	7.85	0.94	acrylic
4	8.059	0.99	acrylic
5	8.164	1.02	acrylic
6	8.269	1.04	acrylic
7	8.373	1.07	acrylic
8	8.478	1.11	acrylic
9	8.583	1.127	acrylic
10	8.687	1.15	acrylic
11	7.326	0.82	sand paper
12	7.641	0.89	sand paper
13	7.85	0.94	sand paper
14	8.059	0.99	sand paper
15	8.164	1.02	sand paper
16	8.269	1.04	sand paper
17	8.373	1.07	sand paper
18	8.478	1.11	sand paper
19	8.583	1.127	sand paper
20	8.687	1.15	sand paper

a digital video recorder was used to capture color images for better image processing. For segregation analysis, the color images were converted to grayscale at a digitized grayscale level range of 0–255, which is appropriate for differentiating between the black (4 mm) and white (2 mm) particles. These images were digitally stored in computer files.

Furthermore, the particle velocities were measured and their granular temperatures were calculated. A high-speed CMOS camera (IDT Y-3 Plus, Monochrome) with a speed of 2000 fps and a resolution of 1280×1024 pixels was used to record the sequential motion of the granular flows during the experiments, which were illuminated by two high-luminance LED lamps (100 W, 6000 K). The digital images were then transferred to a personal computer for further analysis and the shift of each tracer particle in every pair of consecutive images was calculated [31], using cross-correlation technique.

In the calculations, the whole system was divided into several subregions. The ensemble average velocities in each bin were averaged from approximately 750 to 1500 tracer particles (6000 frames):

$$\langle u_i \rangle = \frac{\sum_{k=1}^{N_i} u_{ki}}{N_i} \quad (1)$$

$$\langle v_i \rangle = \frac{\sum_{k=1}^{N_i} v_{ki}}{N_i} \quad (2)$$

where $\langle u_i \rangle$ and $\langle v_i \rangle$ denote the ensemble averaged velocities in the x and y directions, respectively, in the i th bin averaged from veloc-

ities from N_i tracer particles. The subscript k represents the k th tracer particle in the i th bin.

The granular temperature T is defined as the specific fluctuation kinetic energy of the granular flow due to the random motion of the particles. It can be used to quantify the kinetic fluctuation energy of the granular flow and is a key property for studying the dynamic behavior of granular flows [32–34]. A granular system behaves more like a liquid or a gas when it has a relatively higher granular temperature. In a quasi-2D system, the granular temperature in the i th bin can be calculated by:

$$T_i = \frac{\langle u_i'^2 + v_i'^2 \rangle}{2} \quad (3)$$

where u' and v' denote the fluctuation velocities in the i th bin, which are defined as the RMS deviations between the local velocities and the ensemble averaged velocities.

3. Results and discussion

In this section, the results of the experiments are presented and discussed. Table 1 shows the two operational parameters of the system (rotation speed and material of the side walls) which have a significant impact on the segregation process and the flow behavior of the particles. The other parameters were retained.

Images of the arrangement structure of bicolor particles in the double-walled rotating drum were recorded in order to measure the long time-scale segregation behavior of binary-sized mixture. We employed a Sony HDR-XR550 camera with a speed of 30 frames per second and a spatial resolution of 1920×1080 pixels to record the flow images. For each case, more than 1 h of recorded data was used to determine the revolution of the particle segregation. Fig. 2 shows the segregation state at different time revolutions of the double-walled rotating drum with acrylic side walls. The drum was rotated clockwise at a frequency of 7.326 rad/s. At the beginning of each experiment, two different-sized particles (differentiated by color) were placed in the system by random packing to ensure that the initial state was nearly well mixed, as shown in Fig. 2(a). When the mixture was energized by rotation, mixing and segregation progressed simultaneously until both particles achieved a state of equilibrium. As the time revolution increased, ring-like spin segregation began to appear, as shown in Fig. 2(b) and (c). Fig. 2(d) shows the final stable-state segregation pattern after 1260 s. Owing to the percolation effect, smaller particles would fall into voids in between larger particles to form a highly concentrated ring near the inside wall, whereas bigger particles were pushed toward the outside wall.

The degree of particle segregation in the binary mixture can be quantified by a segregation index, as defined by Ciamarra et al. [35], given by:

$$\chi = 2 \frac{h_b - h_s}{h_b + h_s} \quad (4)$$

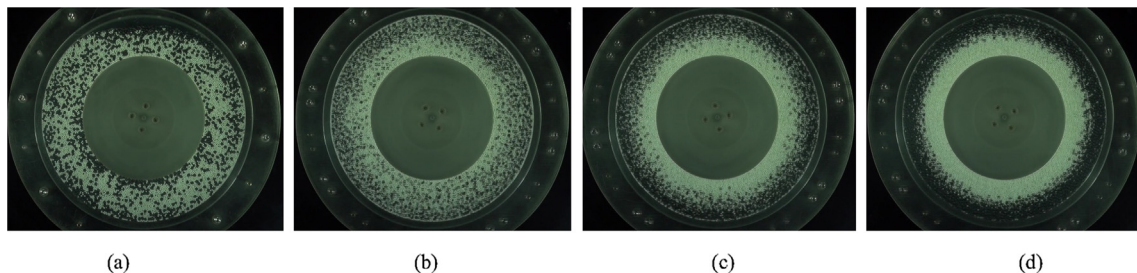


Fig. 2. Experimental images of the rotating drum after (a) 0 s, (b) 120 s, (c) 300 s, and (d) 1260 s for the case of acrylic side walls during the segregation process. The drum is rotated clockwise at a frequency of 7.326 rad/s.

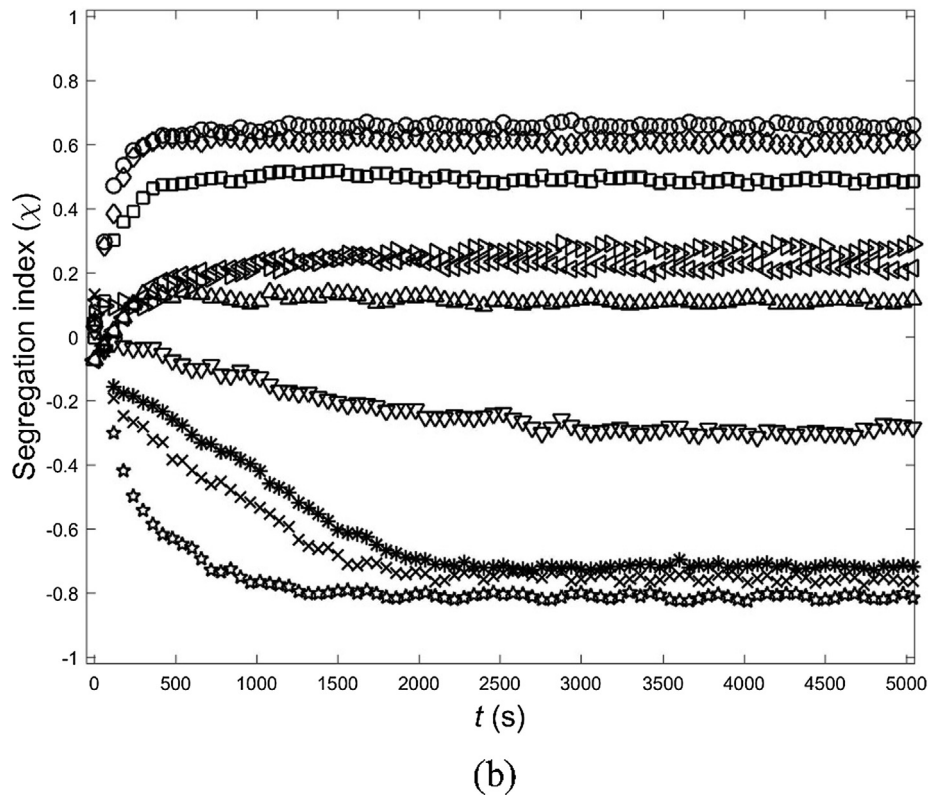
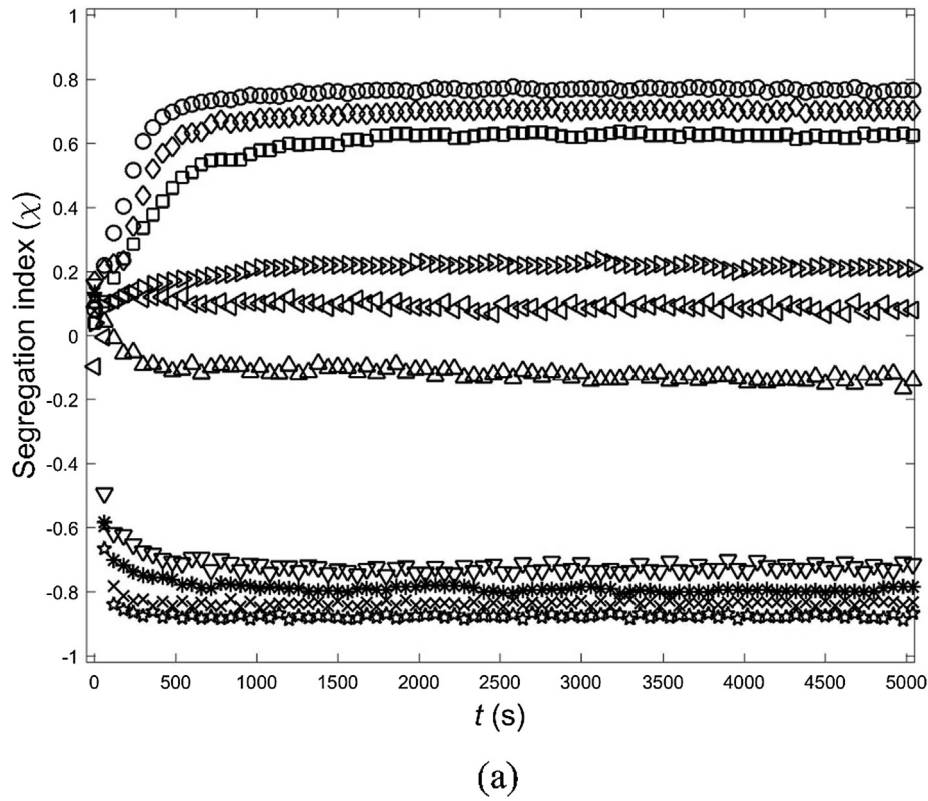


Fig. 3. Variation of segregation index with time revolutions at different rotation speeds for (a) acrylic side walls, and (b) side walls covered by sandpaper. Symbols: \circ , $\omega = 7.326$ rad/s; \diamond , $\omega = 7.641$ rad/s; \square , $\omega = 7.85$ rad/s; \triangleright , $\omega = 8.059$ rad/s; \triangleleft , $\omega = 8.164$ rad/s; Δ , $\omega = 8.269$ rad/s; ∇ , $\omega = 8.373$ rad/s; $*$, $\omega = 8.478$ rad/s; \times , $\omega = 8.583$ rad/s; and \star , $\omega = 8.687$ rad/s.

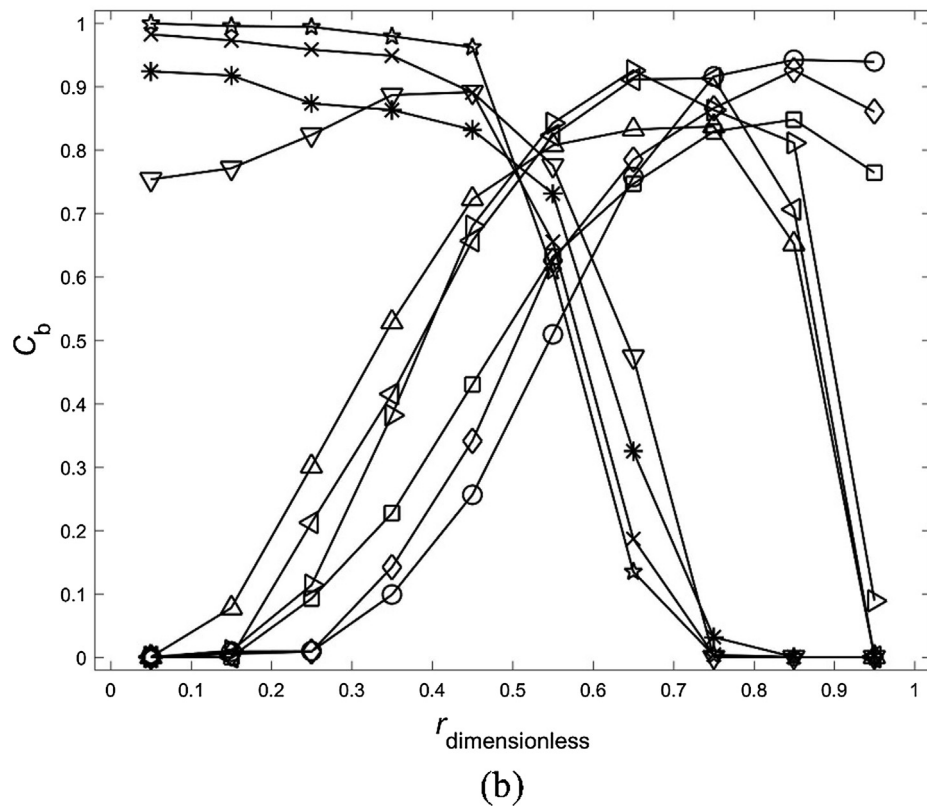
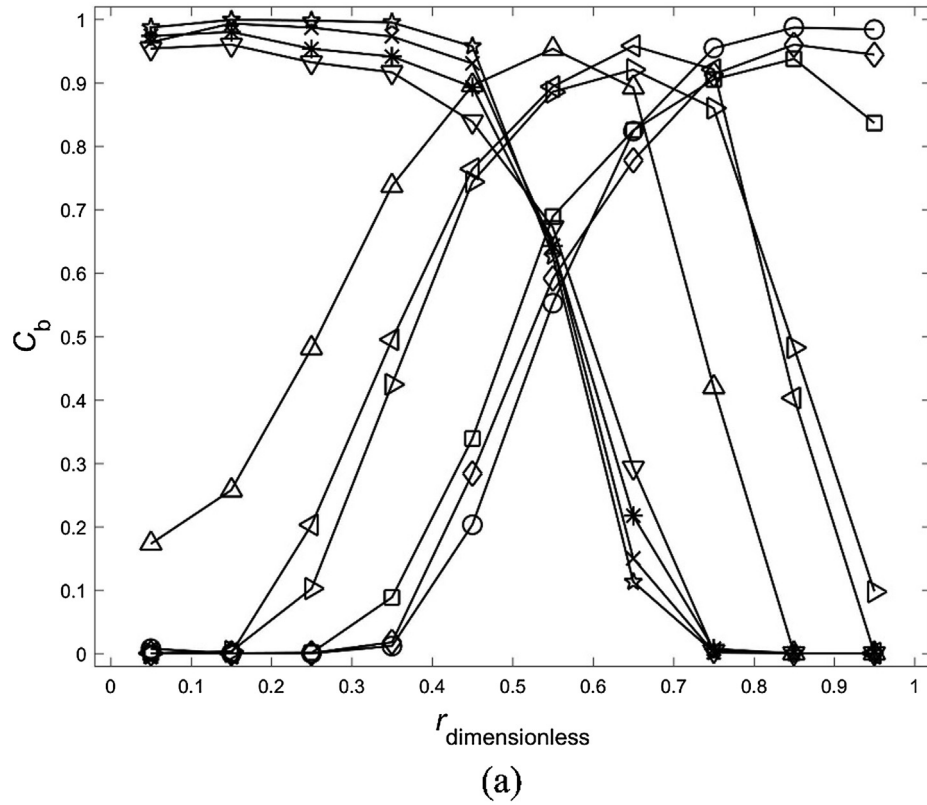


Fig. 4. Variation of the local concentration of bigger particles (C_b) with scaled radial distance ($r_{\text{dimensionless}}$) for the drum (a) with acrylic side walls, and (b) side walls covered with sandpaper, in bidisperse granular systems. Symbols: \circ , $\omega = 7.326$ rad/s; \diamond , $\omega = 7.641$ rad/s; \square , $\omega = 7.85$ rad/s; \triangleright , $\omega = 8.059$ rad/s; \triangleleft , $\omega = 8.164$ rad/s; Δ , $\omega = 8.269$ rad/s; ∇ , $\omega = 8.373$ rad/s; $*$, $\omega = 8.478$ rad/s; \times , $\omega = 8.583$ rad/s; and \star , $\omega = 8.687$ rad/s.

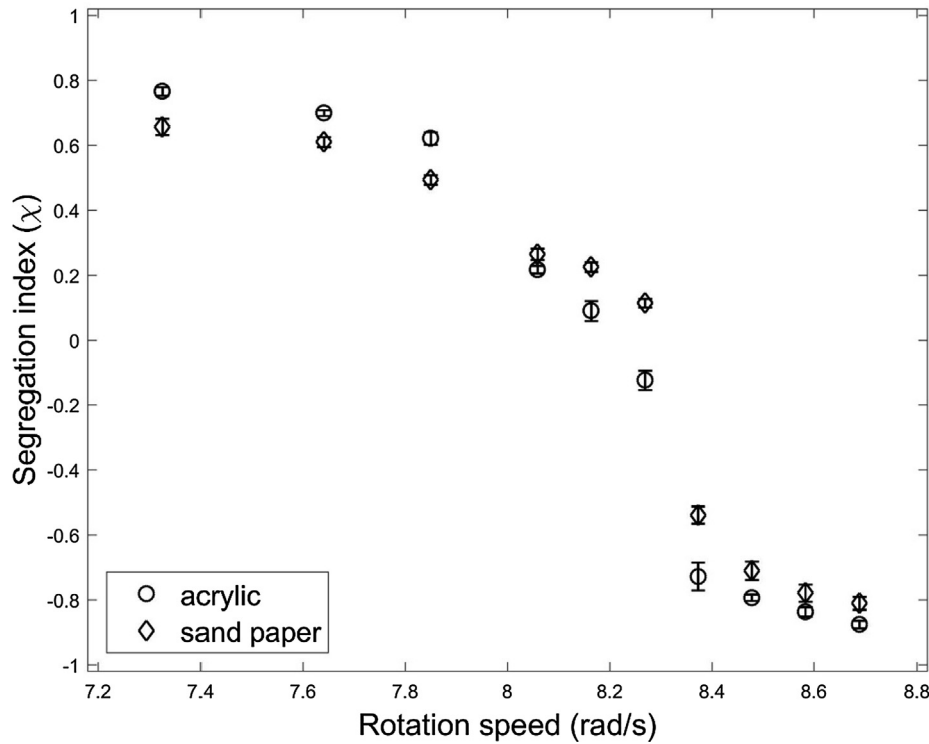


Fig. 5. Segregation index (χ) of the steady state for different side wall conditions at various rotation speeds.

where h_b and h_s are the centers of mass of the bigger particles and the smaller particles, respectively. The position of the i species of particles can be written as:

$$h_i = \frac{\sum_{i=1}^{N_i} \mathbf{d}_i}{N_i} \quad (5)$$

where \mathbf{d}_i is the radial distance between the centroid of the particle and the inside wall of the drum and N is the total number of the i species of particles. The segregation index varies from -1 to 1 . It is larger than zero as the bigger particles move close to the outside wall (known as “Brazil-nut effect”) and less than zero as they move close to the inside wall (known as “reverse Brazil-nut effect”).

The degree of segregation varied as the rotation speed changed from 7.326 to 8.687 rad/s for the two different side walls, as shown in Fig. 3. For the initially almost-mixed loading configuration, the segregation index at $t=0$ was zero for all cases and gradually decreased or increased with time until it reached a stable value (χ_{final}). The asymptotic constant value of the segregation index after 200–800 s depended on the rotation speed. The results also showed that the time required to reach steady state increased with faster rotation speed at the BNE state. However, less time was required to separate the particles by percolation as the rotation speed increased at the RBNE state. Moreover, the particles required more than 1000 s to reach steady state at the RBNE state when the drum side walls were covered with sandpaper. The flow was usually in a complete mixing state when the segregation index $\chi \approx 1$. However, when $Fr \approx 1$, although the segregation index was close to zero and was almost constant with the time revolution, the segregation patterns between the steady and the initial states were different. This particular phenomenon will be discussed in the subsequent paragraphs.

In order to understand particle distribution in the drum, we measured the variation of the black (4 mm) pixel concentration with the scaled radial distance ($r_{\text{dimensionless}} = r - R_i/R_o - R_i$), where

R_i and R_o are the radii of the inside and outside walls, respectively, and r is the radial position, with $r=0$ in the drum center. The larger concentration of the distribution of one kind of particles caused larger local concentration C_b , such that the segregation behavior was more obvious. The rotation drum was a quasi-2D piece of equipment, where the concentration of the bigger (black) particles was determined by the area they occupied. We divided the space between the inside and the outside drum walls into 10 annular cells along the radial direction. As the bigger particles were close to the outside wall, the local concentration was approximately 1 at a scaled radial distance $r_{\text{dimensionless}} = 1$. In contrast, as the bigger particles approached the inside wall, the local concentration was approximately 1 at $r_{\text{dimensionless}} = 0$. Fig. 4(a) shows the variation of local concentration distribution of bigger particles with scaled radial distance at different rotation speeds in a drum with acrylic side walls. At low rotational speed ($Fr < 1$), the bigger particles moved toward the outside wall while the smaller particles migrated to the inside wall. However, a completely opposite scenario was observed at high rotational speed ($Fr > 1$). A similar trend was also observed in Fig. 4(b). Particle fluctuations and interactive collisions were stronger with the drum side walls covered with sandpaper, which did not lead to well segregation condition. At $Fr \approx 1$, three ring-like spin segregation patterns were observed in the radial direction. Bigger particles were concentrated in the ring space in the middle of the granular bed, whereas the smaller particles occupied the space near the outside and inside walls. This phenomenon is known as “double segregation effect (DSE).” These segregation patterns could be observed in both side wall conditions. At the DSE state, the radial position changed while the peak values and concentration width were similar.

Fig. 5 shows a plot of the final segregation index (χ_{final}) indicating its dependence on rotation speeds for both side wall types. This index did not decrease monotonically with the rotation speed. In

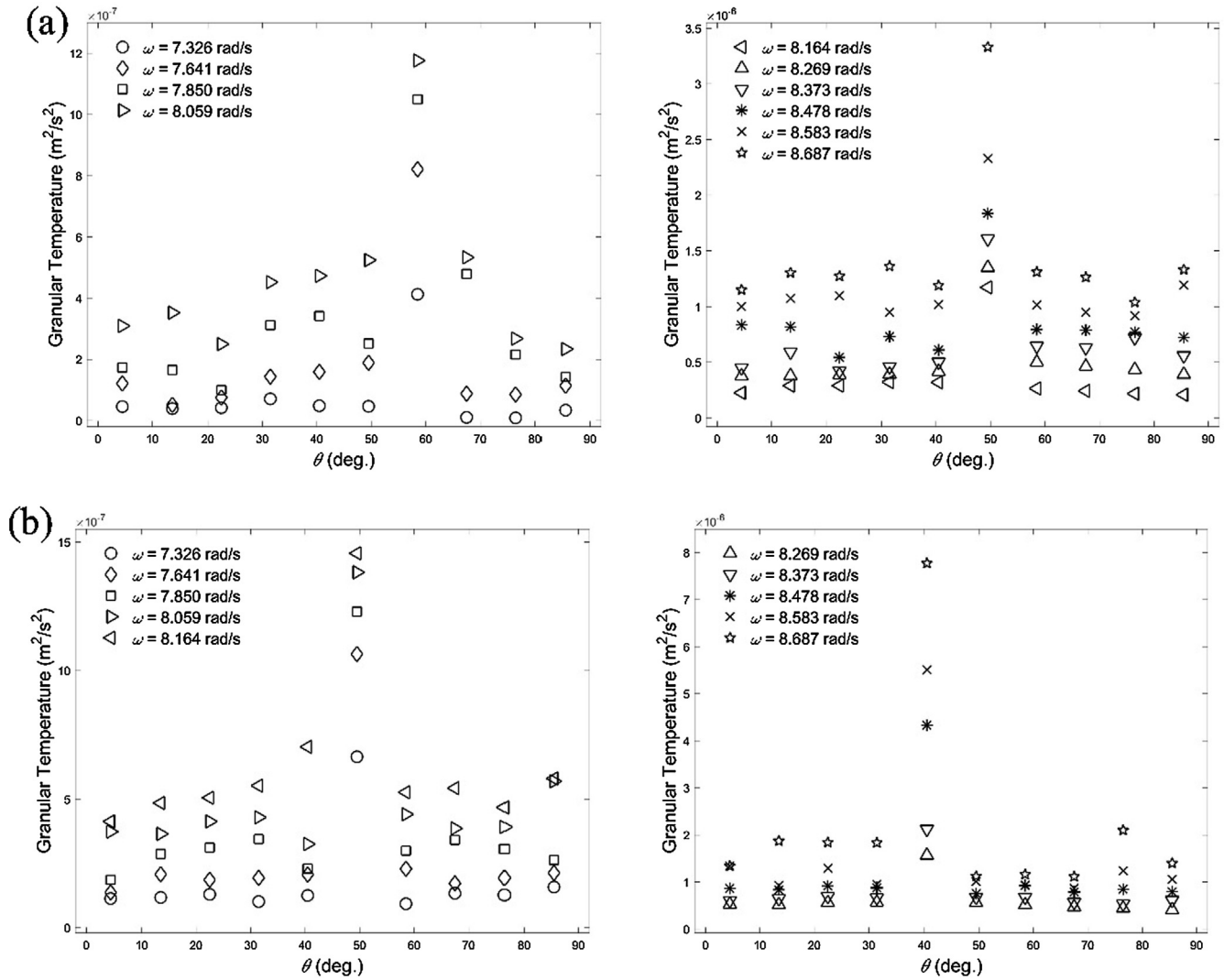


Fig. 6. Distribution of granular temperature with angle from the horizontal line at low (left) and high (right) rotational speeds for (a) acrylic side walls, and (b) side walls covered with sandpaper.

the case of acrylic side walls, the maximum segregation index was observed at a low rotational speed, $\omega = 7.326$ rad/s. When χ was larger than zero and the segregation pattern yielded BNE, the segregation index increased with the decrease of rotation speed. Conversely, the segregation index decreased to less than zero with a higher rotation speed at the RBNE state. For rotational speeds within 7.85–8.373 rad/s, the segregation pattern changed from either BNE or RBNE to DSE segregation pattern. However, all results showed that the absolute values of the segregation index for the drum side walls covered with sandpaper were lower than that of the drum with acrylic side walls at a low or high rotation speed. Thus, the rotation speed significantly influenced the RBNE more than the BNE does.

The granular temperature is a key property for describing the flow of granular materials [32]. It plays the same role as the thermodynamic temperature in gases. The magnitude of the granular temperature depends on the net system energy calculated by subtracting the dissipative energy from the energy input by external sources. The energy of the system gets dissipated due to inelastic collisions as well as fractional and cohesive effects.

The rotating drum used in this study was almost full. Thus, most particles moved at the same radial position, as a solid rotated within a drum. If the rotation of the drum is clockwise, interactions between particles would only occur at the first quadrant of the system. Fig. 6 shows the change in the granular temperature with respect to the angle from the horizontal line (x -axis, Fig. 1), for different rotation speeds at both acrylic and sandpaper side wall conditions. At high rotation speed, the granular temperature significantly changed at the azimuthal angle range of 45–54°, which implied stronger particle motions and interactive collisions. At low rotational speed, the highest granular temperature was observed at azimuthal angles 54–63°, as the inertial force and the force resisting the sliding force due to gravity decreased with decreasing drum rotation speed. Furthermore, there was an increase in the force that resisted the sliding force resulting from gravity as the side wall was changed from acrylic to sandpaper. Therefore, the lower azimuthal angles at which the highest granular temperature occurred, as shown in Fig. 6(b), were all higher than those in Fig. 6(a), given the same drum rotation speed. For instance, the highest granular temperature for a rotation speed of

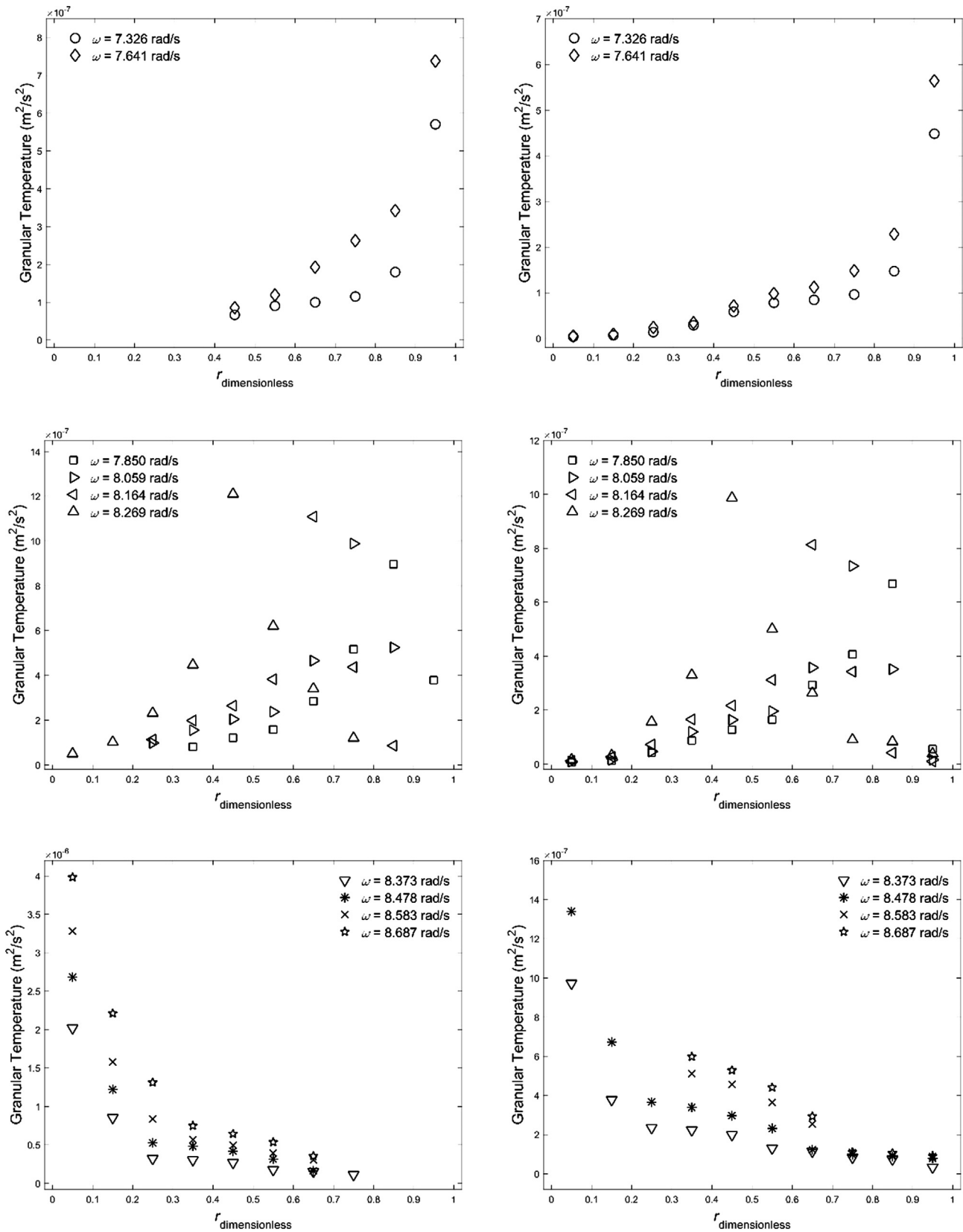


Fig. 7. Distribution of granular temperature with scaled radial direction. The segregation mechanisms are BNE, DSE, and RBNE from top to bottom. The figures in the left-hand column show granular temperature profiles of bigger particles, and those on the right show the profiles of smaller particles. Drum side walls are acrylic.

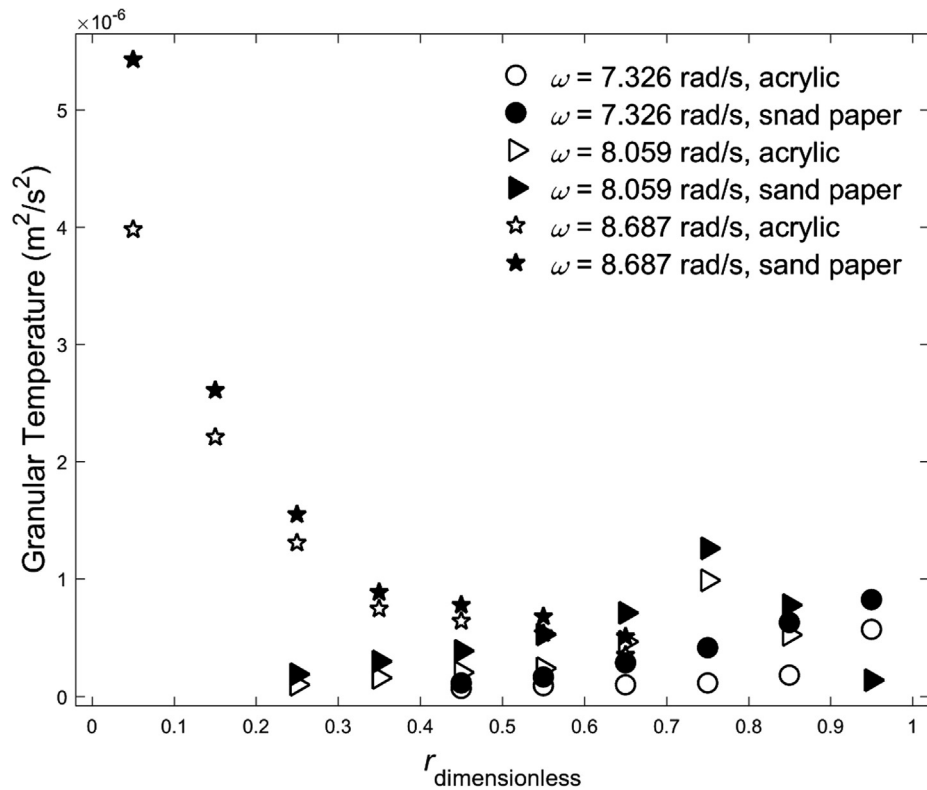


Fig. 8. Relation between the granular temperature of bigger particles and scaled radial distance for different side walls at rotation speeds (ω) of 7.326, 8.059, and 8.687 rad/s.

8.687 rad/s for an acrylic side wall was approximately eight times the highest granular temperature for a rotation speed of 7.326 rad/s. Besides, the highest granular temperature for a rotation speed of 8.687 rad/s for a sandpaper side wall was approximately 11 times the highest granular temperature for a rotation speed of 7.326 rad/s. In other words, the rotational speed had a greater influence on the granular temperature for the drum side wall covered with sandpaper.

Furthermore, gravitational and centrifugal forces played important roles in the granular dynamics inside the rotating drum. At $Fr < 1$, the gravitational force dominated the dynamic properties of the particles. In this case, the inside wall could be regarded as the bottom such that the flowing layer occurred near the outside wall. At $Fr > 1$, the centrifugal force had a more dominant influence, thereby causing particles adjacent to the inside wall to exhibit a flowing layer while the outside wall became the bottom region.

Fig. 7 shows the granular temperature profiles for the mixtures of beads at different rotation speeds using an acrylic side wall. Since the granular temperature was measured in the drum after the flow had reached a steady state, particle segregation indicated the absence of bigger (or smaller) particles at some radial positions. For both of these bidisperse mixture granular flows, the granular temperature decreased with the radial direction from the outside wall at a low rotation speed. At high rotation speed, a completely opposite trend was observed, with the granular temperature highest near the inside wall. Moreover, the granular temperature of the bigger particles was generally higher than that of the smaller particles at the same radial position. A higher granular temperature indicates stronger interactive collisions and fluctuations, where the large mean free path causes larger voids between bigger particles, which is useful during a segregation process. Furthermore, the granular temperature increased with increasing rotation speed as more energy was introduced into the granular

system, thereby generating a higher shear rate. Increased rotation speeds caused stronger particle motions and more interactive collisions due to higher shear rate, which led to a higher granular temperature. At $Fr \approx 1$, different forces dominated at various radial positions, whereas the flowing layer (interaction region) of the particles occurred in the middle of the ring space where the highest granular temperature could be observed. Simultaneously, the peak values of the granular temperature moved toward the inside wall at a higher rotation speed.

Fig. 8 shows the distribution of the granular temperature with the radial direction from the inside wall of both side walls, at rotation speeds of 7.326, 8.059, and 8.687 rad/s. As explained above, particle fluctuations and interactive collisions were stronger with the drum side walls covered with sandpaper. Similarly, the granular temperature for the drum covered with sandpaper was higher than that for the drum with an acrylic side wall at each rotation speed. Additionally, the material of the side wall had a greater degree of influence on the granular temperature at high rotation speeds. Comparing Figs. 7 and 8 with Fig. 5, the radial position at which the highest granular temperature occurred was the point where the bigger particles accumulated, due to a large mean free path between the particles at this position. Thus, small particles fell through the voids between the bigger particles and moved toward the outside (inside) walls.

4. Conclusions

In this study, experiments were performed to investigate the phenomena of particle segregation in a double-walled rotating drum with side walls of different type and different rotation speed. The results indicated that the rotation speed has a significant influence on the segregation of binary-size mixtures granular flows.

The particle exchange and segregation behavior occurred in the upper right-hand corner (the first quadrant of the system). At this time, the gravitational force and the centrifugal force co-exist in this system. Competition with each other will cause different final segregation situations. Thus, several novel results can be found in this research. When the gravitational force dominated the dynamic properties of the particles ($Fr < 1$), the segregation index increased with decreasing rotation speed, where bigger particles moved to the outside wall and smaller particles migrated to the inside wall, also known as the BNE state. When the centrifugal force dominated the dynamic properties of the particles ($Fr > 1$), the segregation index was less than zero, and the segregation pattern was RBNE state. Meanwhile, the DSE state occurred at $Fr \approx 1$, where segregation was close to zero, as in the case of complete mixing. However, bigger particles were concentrated in the ring space in the middle of the granular bed. Here, the effects of gravitational force and centrifugal force are similar. The results of this study for different radial segregation behavior of particles in the rotating drum can be used in many industries. For example, it can be applied to separate rice from their husks or impurities in the food industry as well as the size grading of sand or segregation between sand and garbage in the sand and gravel industry. Moreover, it also can be used to manufacture functionally graded material of different structural types.

Furthermore, velocity fluctuations in the drum side walls covered with sandpaper are enhanced as particles acquire more energy, thereby leading to a reduction in particle percolation. In other words, stronger interactive collisions between particles, along with higher granular temperatures, cause a not well segregation condition. Moreover, the results indicated that the places where the maximum granular temperature occurs and where particles separate coincide.

Acknowledgement

The authors would like to acknowledge the support from the National Science Council of the R.O.C. for this work through Grants MOST 106-2221-E-008 -053 -MY3.

References

- [1] T. Katayama, E. Aoyama, K. Yamamoto, S. Sakaue, Evaluation of two-component powder mixing by vertical vibration: investigation of powder behavior and mixed state by internal pressure fluctuation, *J. Mater. Process. Technol.* 155–156 (2004) 1571–1576.
- [2] A. Santomaso, M. Olivi, P. Canu, Mechanisms of mixing of granular materials in drum mixers under rolling regime, *Chem. Eng. Sci.* 59 (2004) 3269–3280.
- [3] B.J. McCoy, G. Madras, Cluster kinetics of granular mixing, *AIChE J.* 51 (2005) 406–414.
- [4] H. Masuda, K. Higashitani, H. Yoshida (Eds.), *Powder Technology Handbook*, third ed., CRC Press, Boca Raton, 2006.
- [5] G.G. Pereira, S. Pucilowski, K. Liffman, P.W. Cleary, Streak patterns in binary granular media in a rotating drum, *Appl. Math. Model.* 35 (2011) 1638–1646.
- [6] A. Tripathi, D.V. Khakhar, Rheology of binary granular mixtures in the dense flow regime, *Phys. Fluids* 23 (2011) 113302.
- [7] A.A. Aissa, C. Duchesne, D. Rodrigue, Transverse mixing of polymer powders in a rotary cylinder part I: active layer characterization, *Powder Technol.* 219 (2012) 193–201.
- [8] H. Henein, J.K. Brimacombe, A.P. Watkinson, Experimental study of transverse bed motions in rotary kilns, *Metal Trans. B* 14 (1983) 191–205.
- [9] J. Rajchenbach, Flow in powders: from discrete avalanches to continuous regime, *Phys. Rev. Lett.* 65 (2011) 2221–2224.
- [10] C.M. Dury, G.H. Ristow, Competition of mixing and segregation in rotating cylinders, *Phys. Fluid* 11 (1999) 1387–1394.
- [11] D. Eskin, H. Kalman, A numerical parametric study of size segregation in a rotating drum, *Chem. Eng. Process* 39 (2000) 539–545.
- [12] N. Jain, J.M. Ottino, R.M. Lueptow, Combined size and density segregation and mixing in noncircular tumblers, *Phys. Rev. E* 71 (2005) 051301.
- [13] G.H. Ristow, Particle mass segregation in a 2-dimensional rotating drum, *Europhys. Lett.* 28 (1994) 97–101.
- [14] D.V. Khakhar, A.V. Orpe, S.K. Hajra, Segregation of granular materials in rotating cylinders, *Phys. A* 318 (2003) 129–136.
- [15] N. Jain, J.M. Ottino, R.M. Lueptow, Regimes of segregation and mixing in combined size and density granular systems: an experimental study, *Granul. Matter* 7 (2005) 69–81.
- [16] N. Thomas, Reverse and intermediate segregation of large beads in dry granular media, *Phys. Rev. E* 62 (2000) 961–974.
- [17] M.M.H.D. Arntz, W.K. den Otter, W.J. Briels, P.J.T. Bussmann, H.H. Beffink, R.M. Boom, Granular mixing and segregation in a horizontal rotating drum: A simulation study on the impact of rotational speed and fill level, *AIChE J.* 54 (2008) 3133–3146.
- [18] S.H. Chou, C.C. Liao, S.S. Hsiau, An experimental study on the effect of liquid content and viscosity on particle segregation in a rotating drum, *Powder Technol.* 201 (2010) 266–272.
- [19] S.H. Chou, C.C. Liao, S.S. Hsiau, The effect of interstitial fluid viscosity on particle segregation in a slurry rotating drum, *Phys. Fluids* 23 (2011) 083301.
- [20] C.C. Liao, H.W. Lan, S.S. Hsiau, Density-induced granular segregation in a slurry rotating drum, *Int. J. Multiph. Flow* 84 (2016) 1–8.
- [21] K.M. Hill, G. Gioia, D. Amaravadi, Moon Patterns, Sun Pattern, and Wave Breaking in rotating granular mixtures, *Phys. Rev. Lett.* 93 (2005) 224301.
- [22] I. Zuriguel, J.M.N.T. Gray, J. Peixinho, T. Mullin, Pattern selection by a granular wave in a rotating drum, *Phys. Rev. E* 73 (2006) 061302.
- [23] G.G. Pereira, M.D. Sinnott, P.W. Cleary, K. Liffman, G. Metcalfe, I.D. Suto, Insights from simulations into mechanisms for density segregation of granular mixtures in rotating cylinders, *Granul. Matter* 13 (2011) 53–74.
- [24] C.C. Liao, S.S. Hsiau, H.C. Nien, Density-driven spontaneous streak segregation patterns in a thin rotating drum, *Phys. Rev. E* 89 (2014) 062204.
- [25] G. Metcalfe, L. Graham, J. Zhou, K. Liffman, Measurement of particle motions within tumbling granular flows, *Chaos* (1999) 581–593.
- [26] S. Ahmed, S.E. John, I.D. Suto, G. Metcalfe, K. Liffman, Experimental study of density segregation at end walls in a horizontal rotating cylinder saturated with fluid: friction to lubrication transition, *Granul. Matter* 14 (2012) 319–332.
- [27] L.T. Sheng, W.C. Chang, S.S. Hsiau, Influence of particle surface roughness on creeping granular motion, *Phys. Rev. E* 94 (2016) 012903.
- [28] J.L. Turner, M. Nakagawa, Particle mixing in a nearly filled horizontal cylinder through phase inversion, *Powder Technol.* 113 (2000) 119–123.
- [29] D. Huang, M. Lu, G. Sun, Y. Feng, M. Sun, H. Wu, K. Deng, Ringlike spin segregation of binary mixtures in a high-velocity rotating drum, *Phys. Rev. E* 85 (2012) 031305.
- [30] D. Huang, M. Lu, S. Sen, M. Sun, Y. Feng, A. Yang, Spin Brazil-nut effect and its reverse in a rotating double-walled drum, *Eur. Phys. J. E* 36 (2013) 41.
- [31] S.S. Hsiau, H.W. Jang, Measurements of velocity fluctuations of granular materials in a shear cell, *Exp. Thermal and Fluid Sci.* 17 (1998) 202–209.
- [32] S. Ogawa, Multi-temperature theory of granular materials, *Proceedings of US-Japan Seminar on Continuum-Mechanical and Statistical Approaches in the Mechanics of Granular Materials* (Tokyo 208, 1978).
- [33] C.S. Campbell, Rapid granular flows, *Annu. Rev. Fluid Mech.* 22 (1990) 57–92.
- [34] G. Bunin, Y. Shokef, D. Levine, Frequency-dependent fluctuation–dissipation relations in granular gases, *Phys. Rev. E* 77 (2008) 051301.
- [35] M.P. Ciamarra, M.D. De Vizia, A. Fierro, M. Tarzia, A. Coniglio, M. Nicodemi, Granular species segregation under vertical tapping: effects of size, density, friction, and shaking amplitude, *Phys. Rev. Lett.* 96 (2006) 058001.